

Department of Physics and Astronomy
University of Heidelberg

Bachelor Thesis in Physics
submitted by

Torben Karl Schell

born in Heidelberg (Germany)

2011

A Perturbation Series for the Quantum Kicked Rotor

This Bachelor Thesis has been carried out by Torben Karl Schell at the
Institute for Theoretical Physics in Heidelberg
under the supervision of
Dr. Rémy Dubertrand
and
Dr. Sandro Wimberger

Abstract

We develop a perturbation series for the Quantum Kicked Rotor without gravity close to quantum resonance. Therefore we construct the quantum propagator of this problem in angular space and do a perturbation series of the phase of the multi-dimensional integral expression that gives the time evolved state. Doing this we can calculate these integrals analytically. Subsequently we study the range of validity of this perturbative result by comparison to numerical simulations. Further we look at a kind of two dimensional kicked rotor by treating the case of a periodical change of the kicking strength, when this new period is an integer multiple of the kicking period. For this problem we study the pseudo-classical phase space, in particular the occurrence and stability of fixed points, again close to quantum resonance.

Zusammenfassung

Wir entwickeln eine Störungsreihe für den gravitationsfreien getretenen Quantenrotor in der Nähe einer Quantenresonanz. Für dieses Problem geben wir den Propagator im Winkelraum an. Die Abweichung von der Quantenresonanz behandeln wir als Störung und führen eine Störungsentwicklung der Phase des mehrdimensionalen Integrals durch, das den zeitentwickelten Zustand ergibt. Dadurch können wir das Problem auf analytisch berechenbare Integrale zurückführen. Anschließend untersuchen wir den Gültigkeitsbereich dieser Entwicklung durch Vergleich mit numerischen Simulationen. Des Weiteren betrachten wir eine Art zweidimensionale Erweiterung des getretenen Quantenrotors, indem wir die normalerweise konstante Trittsstärke durch eine sich periodisch ändernde ersetzen. Wir beschränken uns hier auf den Fall, dass diese neue Periode mit der Trittsperiode kommensurabel ist, speziell wählen wir die neue Periode als ein ganzzahliges Vielfaches der alten. Für dieses Problem betrachten wir den pseudo-klassischen Phasenraum, genauer das Auftreten und die Stabilität von Fixpunkten nahe einer Quantenresonanz.

Contents

1	Introduction and Outline	3
2	Preliminaries	5
2.1	The Quantum Propagator	5
2.2	The Quantum Kicked Rotor	6
2.3	Kicked Atoms	7
2.4	Dynamics Near to Resonance: ϵ -classics	8
3	A Perturbation Series for the Quantum Kicked Rotor	9
3.1	Transforming the Propagator	9
3.2	Perturbation Series	11
3.3	Validity of the Simplification in the Perturbation Series	15
4	Technical Aspects	19
4.1	Numerics	19
4.2	Calculation of the Perturbation Series	19
5	Investigation of the Perturbation Series	23
5.1	Results	23
5.2	Time of Validity	23
5.3	Initial Gaussian State in Momentum Space	27
5.4	Fidelity	29
6	2D Kicked Rotor	31
6.1	Classical Description	31
6.2	Quantum Mechanical and ϵ -classical Description	31
6.3	Fixed Points	32
7	Conclusion and Outlook	35
A	The Quantum Propagator - Some Examples	37
A.1	Bouncing Particle Between Two Walls	37
A.2	Particle on a Ring	38
A.3	Shifted Momentum	39
A.4	Initial Velocity	40
A.5	Time Evolution of a Particle in the 1-dim Harmonic Oscillator	40
B	FFT Subroutine	43

1 Introduction and Outline

The kicked rotor model is a quite simple system: a rigid rotor that experiences δ -like gravitational kicks. But even this simple Hamiltonian system shows chaotic behavior and thus can be used as a toy model for chaotic systems. Furthermore there are many systems that can be mapped to this model. Its classical description is given by the standard map which had been made famous by B. Chirikov in 1979 [1]. An intuitive way to study quantum dynamics of chaotic systems is to start from the quantized version of this model: the Quantum Kicked Rotor. Treating the quantum version yielded two new phenomena. First Dynamical Localization [2], which means that the mean energy stops growing after a certain break time. It was shown that this phenomenon is closely linked to Anderson localization in solid state physics [3]. And second the occurrence of quantum resonances at which the mean energy increases ballistically [2]. The Quantum Kicked Rotor is even more interesting since it can be realized in experiment [4]. One experimental realization of the Quantum Kicked Rotor are cold atoms moving along a line being kicked by an periodically switched on and off standing light wave which was realized for a first time in [5]. Newer experiments use Bose-Einstein condensates, e.g. [6].

A powerful tool to investigate the behavior of the Quantum Kicked Rotor close to these resonances are the so called ϵ -classics that have been developed by Fishman, Rebuzzini and Guarneri in 2003 [7]. In the last years this method provided a deeper understanding of the Quantum Kicked Rotor [8]. A straightforward way to treat a system very close to a specific state is to do a perturbation series. In this thesis we will treat the Quantum Kicked Rotor from the quantum propagator point of view. Then we will do a perturbation series starting from the quantum propagator of the Quantum Kicked Rotor and will reduce the complicated multi-dimensional integral to the well-known Gaussian integrals. Having such an approach the first question one should ask is for the range of validity. Therefore we will compare our perturbation theory to numerical simulations which can be performed quite easily for the Quantum Kicked Rotor.

In the past there have been many investigations in quantum chaos and quantum information using fidelity, which is defined as the overlap of two wave functions that develop under slightly different dynamics. This measure of stability was developed since the classical definition of chaos, namely that the difference between two initially neighboring states increases exponentially with time, becomes meaningless when one does the step to quantum systems, where the time evolution is unitary [9]. Because of the importance of this quantity we will check whether our perturbative approach allows stud-

ies about it.

In the last part of this thesis we will expand the simple Quantum Kicked Rotor with a constant kicking strength to a kind of two-dimensional version by discussion of a kicking strength changing periodically in time. This introduces a second time period to the system. For simplicity we will restrict to the special case of commensurable time periods. In particular only the case that the kicking strength will modulate with a time period that is an integer multiple of the period of the kicks. For this case we will study the occurrence of fixed points in the ϵ -classical phase space.

2 Preliminaries

In this chapter we will introduce the theoretical background for our later studies. Therefore we will give a brief overview of some concepts of the quantum propagator formalism. Further we will present the Quantum Kicked Rotor and the concrete realization we are interested. We will explain what quantum resonances are and how ϵ -classics allow us to study the behavior close to this resonances.

2.1 The Quantum Propagator

The quantum propagator is a solution of the Schrödinger equation with very specific initial conditions:

$$\left(i\hbar \frac{\partial}{\partial t} - \hat{H} \right) K(x, t|x_0, 0) = 0, \quad (1)$$

$$\lim_{t \rightarrow 0} K(x, t|x_0, 0) = \delta(x - x_0). \quad (2)$$

The propagator formalism comes from the theory of path integration, which was developed by R. Feynman [10]. The propagator includes the whole information on the dynamics of the system. Once it is known, we can get the time evolution of an initial state $\Psi(x_0, 0)$ by evaluating the integral

$$\Psi(x, t) = \int_{-\infty}^{\infty} dx_0 K(x, t|x_0, 0) \Psi(x_0, 0). \quad (3)$$

We can treat the propagator as transition amplitude and express it in terms of the more familiar unitary time evolution operator \hat{U} :

$$K(x, t) = \langle x, t | \hat{U} | x_0, 0 \rangle \quad (4)$$

$$= \langle x, t | \mathcal{T} \exp \left\{ -\frac{i}{\hbar} \int_0^t dt' \hat{H}(t') \right\} | x_0, 0 \rangle. \quad (5)$$

Starting from the well-known propagator of a free particle [11, 12]

$$K_f(x, t|x_0, 0) = \left(\frac{m}{2\pi i \hbar t} \right)^{\frac{1}{2}} \exp \left(\frac{im(x - x_0)^2}{2\hbar t} \right) \quad (6)$$

we will study some simple examples to get an intuition of the quantum propagator formalism in appendix A.

2.2 The Quantum Kicked Rotor

First let us consider the classical kicked rotor: a single particle of unit mass on a ring (unit circle). This particle is kicked periodically with a force k in a fixed direction. A single kick is considered to be δ -like.

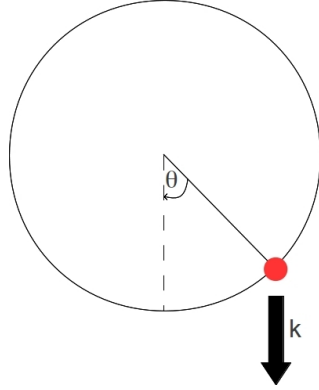


Figure 1: Kicked Rotor.

The Hamiltonian of this problem reads:

$$H(p, \theta, t) = \frac{p^2}{2} + k \cos(\theta) \sum_{\nu=-\infty}^{+\infty} \delta(t - \nu\tau), \quad (7)$$

where p is the angular momentum, τ the time period of the kicking, k the kicking strength and the position on the ring is characterized by the angle θ . Calculating Hamilton's equation of motion from the Hamiltonian above and integration over one period gives

$$p_{\nu+1} = p_{\nu} + k \sin \theta_{\nu+1} \quad (8)$$

$$\theta_{\nu+1} = \theta_{\nu} + p_{\nu}\tau \pmod{2\pi}. \quad (9)$$

By introducing $J = p\tau$, one finds the so called Standard Map [1]:

$$J_{\nu+1} = J_{\nu} + \kappa \sin \theta_{\nu+1} \quad (10)$$

$$\theta_{\nu+1} = \theta_{\nu} + J_{\nu} \pmod{2\pi}, \quad (11)$$

with the stochasticity parameter or classical kicking strength $\kappa = k\tau$. The phase space of this problem is a cylinder. But the map is 2π -periodic in momentum as well. Therefore the phase space structure can be taken periodic in the momentum direction, which gives a torus. In the quantum version we replace

the classical observables p and θ by operators, which results in quantization of the momentum in multiples of \hbar . The Floquet operator (one period time evolution operator) from right after a kick till right after the next one is given by:

$$\hat{U} = e^{-\frac{i}{\hbar}k \cos(\hat{\theta})} e^{-\frac{i}{\hbar} \frac{\hat{p}^2}{2} \tau}. \quad (12)$$

The factorization in a free and a kicking part is only possible due to the δ -like kicking potential. This fact makes the Quantum Kicked Rotor amenable to analytical treatment and simplifies numerical computations as explained in section 4.1.

2.3 Kicked Atoms

Motivated by the experimental implementation [4], we are interested in a particle moving along a line instead of a circle. More precisely an atom moving on a line being kicked by a periodic potential, which is created by a standing laser wave, that is switched on and off periodically in time. The idealized δ -like kicks can be approximated in experiments if the time for which the laser is on is chosen such that the atom's motion during this time is negligible. The Hamiltonian reads [13]:

$$H'(p, x, t) = \frac{p^2}{2m} + V_0 \cos(2\pi \frac{x}{a}) \sum_{\nu=-\infty}^{\infty} \delta(t - n\tau). \quad (13)$$

We set $m = 1$ and identify the amplitude of the potential V_0 with the kicking strength k . Since our Hamiltonian is periodic in x , Bloch's theorem holds and we can express the eigenfunction of the stationary Schrödinger equation as combinations of plane waves and periodic functions:

$$\Psi(x) = \int_0^1 d\beta \psi_\beta(x) e^{i\beta x}, \quad (14)$$

where $\psi_\beta(\theta) = \psi_\beta(\theta + 2\pi)$. The momentum of one Bloch wave is

$$p = n + \beta, \quad (15)$$

where n is an integer and $\beta \in [0, 1)$. Here and below we set $\hbar = 1$. Thus our single particle along a line can be mapped onto a family of so called β rotors. The quasi-momentum β is for each rotor a constant of motion. The Floquet operator for one single β -rotor reads

$$\hat{U}_\beta = e^{-ik \cos(\hat{\theta})} e^{-i \frac{(\mathcal{N} + \beta)^2}{2} \tau}, \quad (16)$$

where $\hat{\mathcal{N}} = -i\frac{d}{d\theta}$ with periodic boundary conditions. An special case is the behavior of the system, if the free time evolution part in the Floquet operator equals unity. This means that N kicks of strength k are equal to one kick of strength Nk . In this regime the momentum grows linear in time and therefore the energy increases quadratically. The condition for this is:

$$\tau = 2\pi l, \quad l \in \mathbb{N}, \beta = \frac{1}{2} + \frac{j}{l} \quad j = 0, 1, \dots, l-1. \quad (17)$$

These resonances of the system, that do not occur in the classical kicked rotor, are known as quantum resonances.

2.4 Dynamics Near to Resonance: ϵ -classics

A powerful method to study dynamics close to a quantum resonance was developed by S. Fishman, I. Guarneri and L. Rebuzzini in [7]. We consider $\tau = 2\pi l + \epsilon$, with integer l and a small deviation from the resonance ϵ . After rescaling $\tilde{k} = |\epsilon|k$, $\hat{I} = \hat{\mathcal{N}}|\epsilon|$ and using $e^{-i\pi l \hat{\mathcal{N}}^2} = e^{-i\pi l \hat{\mathcal{N}}}$ the Floquet operator reads:

$$\hat{U}_\beta = e^{-\frac{i}{|\epsilon|}\tilde{k}\cos(\hat{\theta})} e^{-\frac{i}{|\epsilon|}\left(\frac{\hat{I}^2}{2\text{sgn}(\epsilon)} + \hat{I}(\pi l + \beta\tau)\right)} e^{-\frac{i}{2}\beta^2\tau}. \quad (18)$$

Here $|\epsilon|$ takes over the role of \hbar . For the free evolution we find an effective Hamiltonian

$$\tilde{H} = \frac{I^2}{2\text{sgn}(\epsilon)} + I(\pi l + \beta\tau). \quad (19)$$

This corresponds to the case of an initial velocity, which is treated in A.4. Using the result we had for periodic boundary conditions (A.2), the one period propagator ($n^+ \rightarrow (n+1)^+$) for this Hamiltonian is

$$K(\theta, n+1|\theta_0, n) = (2\pi i\epsilon)^{-\frac{1}{2}} e^{-\frac{i}{2}\beta^2\tau} \sum_{\mu \in \mathbf{Z}} e^{\frac{i}{2\epsilon}(\theta - \theta_0 - 2\pi\mu - (\pi l + \beta\tau))^2}. \quad (20)$$

3 A Perturbation Series for the Quantum Kicked Rotor

In this section we develop a perturbation series for the Quantum Kicked Rotor. First we transform the integral expression for the propagated state such that the integration boundaries change from 0 and 2π to $\pm\infty$. For this expression we give a perturbation series up to second order in $\sqrt{|\epsilon|}$ and reduce this multi-dimensional integral under one restricting assumption, which we discuss at the end of this section, to a product of one-dimensional Gaussian integrals that can be evaluated analytically.

3.1 Transforming the Propagator

The time evolved state from $t = n^+$ to $t = (n + 1)^+$ including one kick reads

$$\psi(\theta, t = n + 1) = e^{-ik \cos \theta} \int_0^{2\pi} d\theta_0 K(\theta, t = n + 1 | \theta_0, t = n) \psi(\theta_0, n). \quad (21)$$

For $t = N$ we find by iterating the formula above

$$\begin{aligned} \psi(\theta_N, N) &= (2\pi i \epsilon)^{-\frac{N}{2}} e^{-i\frac{N}{2}\beta^2\tau} \\ &\times \int_0^{2\pi} d\theta_{N-1} \dots \int_0^{2\pi} d\theta_0 \times \sum_{m_1 \dots m_N \in \mathbb{Z}} \exp \left[-ik \sum_{r=1}^N \cos \theta_r \right. \\ &\left. + \frac{i}{2\epsilon} \sum_{j=1}^N [\theta_j - \theta_{j-1} - (\pi l + \tau\beta) - 2\pi m_j]^2 \right] \psi(\theta_0, 0). \quad (22) \end{aligned}$$

From now on we write $\theta_N = \theta$, substitute $\xi = (\pi l + \tau\beta)$ and change variables

$$\eta_j = \theta_j - \theta_{j-1} - \xi \Leftrightarrow \theta_j = \theta - (N - j)\xi - \sum_{l=j+1}^N \eta_l. \quad (23)$$

Thus the bounds change accordingly

$$\int_0^{2\pi} d\theta_{N-1} \dots \int_0^{2\pi} d\theta_0 \rightarrow \int_{-2\pi+\theta-\xi}^{\theta-\xi} d\eta_N \int_{-2\pi-\eta_N+\theta-2\xi}^{-\eta_N+\theta-2\xi} d\eta_{N-1} \dots \int_{-2\pi+\theta-N\xi-\sum_{i=2}^N \eta_i}^{\theta-N\xi-\sum_{i=2}^N \eta_i} d\eta_1, \quad (24)$$

since $\eta_j = -\theta_j + \theta - (N-j)\xi - \sum_{l=j+1}^N \eta_l$ for $1 \leq j \leq N$.
Therefore we get for one integral

$$\sum_{m_j \in \mathbb{Z}} \int_{\alpha_j - 2\pi}^{\alpha_j} e^{-ik \sum_{r=1}^N \cos[\theta - (N-r)\xi - \sum_{l=r+1}^N \eta_l]} e^{i \frac{(\eta_j + 2\pi m_j)^2}{2\epsilon}} \times \psi \left(\theta - N\xi - \sum_{l=1}^N \eta_l \right) d\eta_j, \quad (25)$$

where α_j is some constant, which we do not need to make explicit here. We set $u_j = \eta_j + 2\pi m_j$ and find

$$\sum_{m_j \in \mathbb{Z}} \int_{\alpha_j + 2\pi(m_j - 1)}^{\alpha_j + 2\pi m_j} \exp \left[-ik \sum_{r=1}^N \cos \left[\theta - (N-r)\xi - \sum_{l=r+1}^N u_l \right] + i \frac{u_j^2}{2\epsilon} \right] \times \psi \left(\theta - N\xi - \sum_{l=1}^N u_l \right) du_j. \quad (26)$$

Since the term $2\pi m_j$ in the arguments of the 2π -periodic functions $\cos(x)$, e^{ix} and the 2π -periodic initial state vanishes we can contract each j -integral to $\int_{-\infty}^{\infty} du_j$ and have

$$\begin{aligned} \psi(\theta, N) &= (2\pi i \epsilon)^{-\frac{N}{2}} e^{-i \frac{N}{2} \beta^2 \tau} \int_{-\infty}^{\infty} du_N \dots \int_{-\infty}^{\infty} du_1 \\ &\times \exp \left[-ik \sum_{j=1}^{N-1} \cos \left[\theta - (N-j)\xi - \sum_{l=j+1}^N u_l \right] \right. \\ &\left. + \frac{i}{2\epsilon} \sum_{j=1}^N u_j^2 \right] \psi \left(\theta - N\xi - \sum_{l=1}^N u_l \right). \end{aligned} \quad (27)$$

Finally we substitute $x_j = \frac{u_j}{\sqrt{|\epsilon|}}$ and get

$$\begin{aligned} \psi(\theta, N) &= (2\pi i \operatorname{sgn}(\epsilon))^{-\frac{N}{2}} e^{-i \frac{N}{2} \beta^2 \tau} \int_{-\infty}^{\infty} dx_N \dots \int_{-\infty}^{\infty} dx_1 \\ &\times e^{-ik \sum_{j=1}^{N-1} \cos \left[\theta - (N-j)\xi - \sqrt{|\epsilon|} \sum_{l=j+1}^N x_l \right]} \\ &\times e^{\frac{i}{2} \operatorname{sgn}(\epsilon) \sum_{j=1}^N x_j^2} \psi \left(\theta - N\xi - \sqrt{|\epsilon|} \sum_{l=1}^N x_l \right). \end{aligned} \quad (28)$$

3.2 Perturbation Series

We start with the quantum propagator

$$\begin{aligned} \psi(\theta, N) &= (2\pi \operatorname{sgn}(\epsilon) i)^{-\frac{N}{2}} e^{-i\frac{N}{2}\beta^2\tau - ik \cos \theta} \int_{-\infty}^{\infty} dx_N \dots \int_{-\infty}^{\infty} dx_1 \\ &\times e^{-ik \sum_{j=1}^{N-1} \cos(\theta - (N-j)\xi - \sqrt{|\epsilon|} \sum_{l=j+1}^N x_l)} \\ &\times e^{\frac{i}{2} \operatorname{sgn}(\epsilon) \sum_{j=1}^N x_j^2} \psi \left(\theta - N\xi - \sqrt{|\epsilon|} \sum_{l=1}^N x_l \right), \end{aligned} \quad (29)$$

where

$$\xi = \pi l + 2\pi l\beta + \operatorname{sgn}(\epsilon)|\epsilon|\beta = \gamma + \beta \operatorname{sgn}(\epsilon)|\epsilon|, \quad \gamma = \pi l(1 + 2\beta). \quad (30)$$

Since we are interested in the behavior near to resonances (i.e. $|\epsilon|$ small), we expand our expression in orders of $\delta = \sqrt{|\epsilon|}$. An expansion in orders of ϵ is not possible because this would yield terms like $|\epsilon|^{-\frac{1}{2}}$ that have to be evaluated at $|\epsilon| = 0$. As initial state we consider a plane wave

$$\psi(\theta, 0) = e^{in_0\theta}, \quad (31)$$

where we have chosen the normalization such that the norm in momentum space is 1 and the normalization factor of the Fourier transform is given to the normal Fourier transform.

The propagator of our system has a typical phase structure that results from the unitary time evolution operator. In this picture each energy eigenstate evolves with a specific phase and the phase structure in combination with the hermiticity of the Hamilton operator guaranties an unitary time evolution. To keep this phase structure of the propagator we will not do a classical Taylor expansion of the whole term, but only of the exponents. For simplicity we will neglect the global phase

$$e^{-i\frac{N}{2}\beta^2\tau} \quad (32)$$

in the following calculation. Thus there are two terms, which we have to expand:

$$f(\delta) = \cos \left(\theta - (N-j)\gamma - (N-j)\operatorname{sgn}(\epsilon)\delta^2\beta - \delta \sum_{l=j+1}^N x_l \right) \quad (33)$$

$$g(\delta) = -N\operatorname{sgn}(\epsilon)\delta^2\beta - \delta \sum_{l=1}^N x_l. \quad (34)$$

We find (the second one is already given in orders of δ)

$$\begin{aligned}
f(\delta) &= \cos(\theta - (N-j)\gamma) + \delta \left[\sum_{l=j+1}^N x_l \sin(\theta - (N-j)\gamma) \right] \\
&+ \frac{\delta^2}{2} \left[- \left(\sum_{l=j+1}^N x_l \right)^2 \cos(\theta - (N-j)\gamma) \right. \\
&\left. + 2(N-j) \operatorname{sgn}(\epsilon) \beta \sin(\theta - (N-j)\gamma) \right] + O(\delta^3) \quad (35)
\end{aligned}$$

$$g(\delta) = -\delta \sum_{l=1}^N x_l - \delta^2 \operatorname{sgn}(\epsilon) N \beta. \quad (36)$$

Using terms up to second order the propagated wave function reads

$$\begin{aligned}
\psi(\theta, N) &= (2\pi \operatorname{sgn}(\epsilon) i)^{-\frac{N}{2}} e^{-ik \cos(\theta)} \\
&\times \int_{-\infty}^{\infty} dx_N \dots \int_{-\infty}^{\infty} dx_1 e^{-ik \sum_{j=1}^{N-1} (\cos[\theta - (N-j)\gamma] + \delta [\sin[\theta - (N-j)\gamma] \sum_{l=j+1}^N x_l])} \\
&\times e^{-ik \sum_{j=1}^{N-1} \left(\frac{\delta^2}{2} [-\cos[\theta - (N-j)\gamma] (\sum_{l=j+1}^N x_l)^2 + \sin[\theta - (N-j)\gamma] 2(N-j) \operatorname{sgn}(\epsilon) \beta] \right)} \\
&\times e^{\frac{i}{2} \operatorname{sgn}(\epsilon) \sum_{j=1}^N x_j^2} e^{in_0(\theta - N\delta^2 \operatorname{sgn}(\epsilon) \beta - \delta \sum_{l=1}^N x_l)}. \quad (37)
\end{aligned}$$

Below we will use

$$\sum_{j=1}^{N-1} \left(a_j \sum_{l=j+1}^N x_l \right) = \sum_{j=1}^N \left(x_j \sum_{r=1}^{j-1} a_r \right) \quad (38)$$

with the convention $\sum_{r=1}^0 = 0$ and

$$\sum_{j=1}^{N-1} a_j \left(\sum_{l=j+1}^N x_l \right)^2 = \sum_{j=1}^N \left(x_j^2 \sum_{r=1}^{j-1} a_r \right) + 2 \left[\sum_{j=1}^N x_j \left(\sum_{r=j+1}^N x_r \right) \left(\sum_{s=1}^{j-1} a_s \right) \right]. \quad (39)$$

The argument of the whole exponential e^{arg} is

$$\begin{aligned}
\text{arg} &= -ik \sum_{j=1}^N \left(\cos[\theta - (N-j)\gamma] + \delta \left[\sin[\theta - (N-j)\gamma] \sum_{l=j+1}^N x_l \right] \right) \\
&\quad - ik \sum_{j=1}^{N-1} \left(\frac{\delta^2}{2} \left[-\cos[\theta - (N-j)\gamma] \left(\sum_{l=j+1}^N x_l \right)^2 + \sin[\theta - (N-j)\gamma] 2\text{sgn}(\epsilon)(N-j)\beta \right] \right) \\
&\quad + \frac{i}{2} \text{sgn}(\epsilon) \sum_{j=1}^N x_j^2 + in_0 \left(\theta - N\gamma - N\delta^2 \text{sgn}(\epsilon)\beta - \delta \sum_{l=1}^N x_l \right) \tag{40}
\end{aligned}$$

$$\begin{aligned}
&= -ik \cos(\theta) - ik \left[\sum_{j=1}^{N-1} \left(\cos[\theta - (N-j)\gamma] + \frac{\delta^2}{2} \sin[\theta - (N-j)\gamma] 2\text{sgn}(\epsilon)(N-j)\beta \right) \right] \\
&\quad + in_0(\theta - N\gamma - N\delta^2 \text{sgn}(\epsilon)\beta) - ik\delta \sum_{j=1}^N \left(x_j \sum_{r=1}^{j-1} \sin[\theta - (N-r)\gamma] \right) \\
&\quad + ik \frac{\delta^2}{2} \sum_{j=1}^N \left(x_j^2 \sum_{r=1}^{j-1} \cos[\theta - (N-r)\gamma] \right) \\
&\quad + ik\delta^2 \sum_{j=1}^N \left(x_j \left(\sum_{r=1}^{j-1} \cos[\theta - (N-r)\gamma] \right) \sum_{s=j+1}^N x_s \right) + \frac{i}{2} \text{sgn}(\epsilon) \sum_{j=1}^N x_j^2 - in_0\delta \sum_{l=1}^N x_l \tag{41}
\end{aligned}$$

$$\begin{aligned}
&= -ik \cos(\theta) - ik \left[\sum_{j=1}^{N-1} \left(\cos[\theta - (N-j)\gamma] + \frac{\delta^2}{2} \sin[\theta - (N-j)\gamma] 2\text{sgn}(\epsilon)(N-j)\beta \right) \right] \\
&\quad + in_0(\theta - N\gamma - N\delta^2 \text{sgn}(\epsilon)\beta) + \sum_{j=1}^N \left[-x_j^2 \left(\frac{\text{sgn}(\epsilon)}{2i} + \frac{1}{2i} k\delta^2 \sum_{r=1}^{j-1} \cos[\theta - (N-r)\gamma] \right) \right] \\
&\quad + \sum_{j=1}^N \left[x_j \left(-ik\delta \sum_{r=1}^{j-1} \sin[\theta - (N-r)\gamma] + ik\delta^2 \left(\sum_{r=1}^{j-1} \cos[\theta - (N-r)\gamma] \right) \sum_{s=j+1}^N x_s \right. \right. \\
&\quad \left. \left. - in_0\delta \right) \right]. \tag{42}
\end{aligned}$$

Evaluating the x_j dependent parts, we have for one j

$$\begin{aligned}
& \int_{-\infty}^{\infty} dx_j e^{\sum_{j=1}^N [-x_j^2 (\frac{\text{sgn}(\epsilon)}{2i} + \frac{1}{2i} k\delta^2 \sum_{r=1}^{j-1} \cos[\theta - (N-r)\gamma])]} \\
& \times e^{\sum_{j=1}^N [x_j (-ik\delta \sum_{r=1}^{j-1} \sin[\theta - (N-r)\gamma] + ik\delta^2 (\sum_{r=1}^{j-1} \cos[\theta - (N-r)\gamma]) \sum_{s=j+1}^N x_s - in_0\delta]}] \\
& = (2\pi i)^{\frac{1}{2}} \left(\text{sgn}(\epsilon) + k\delta^2 \sum_{r=1}^{j-1} \cos[\theta - (N-r)\gamma] \right)^{-\frac{1}{2}} \\
& \exp \left(-\frac{i}{2} \left(\text{sgn}(\epsilon) + k\delta^2 \sum_{r=1}^{j-1} \cos[\theta - (N-r)\gamma] \right)^{-1} \times \right. \\
& \times \left[k\delta \sum_{r=1}^{j-1} \sin[\theta - (N-r)\gamma] - k\delta^2 \left(\sum_{r=1}^{j-1} \cos[\theta - (N-r)\gamma] \right) \sum_{s=j+1}^N x_s \right. \\
& \left. \left. + n_0\delta \right]^2 \right), \tag{43}
\end{aligned}$$

where we used

$$\int_{-\infty}^{\infty} dx e^{-Ax^2+Bx} = \sqrt{\frac{\pi}{A}} e^{\frac{B^2}{4A}} \tag{44}$$

for $A \in \mathbf{C} | \text{Re}(A) \geq 0$.

Since $\left(\text{sgn}(\epsilon) + k\delta^2 \sum_{r=1}^{j-1} \cos[\theta - (N-r)\gamma] \right)^{-1} \approx 1$ if the sum does not reach $k^{-1}\delta^{-2}$ and we restricted ourselves to terms up to second order in δ , the squared term in the exponential becomes $\left[k\delta \sum_{r=1}^{j-1} \sin[\theta - (N-r)\gamma] + n_0\delta \right]^2$. That simplifies our calculations a lot because the terms including other x dropped. The validity of this approximation is discussed in 3.3. Thus each x_j -integral results in a term independent of the other x_j 's.

$$\begin{aligned}
& (2\pi i)^{\frac{1}{2}} \left(\text{sgn}(\epsilon) + k\delta^2 \sum_{r=1}^{j-1} \cos(\theta - (N-r)\gamma) \right)^{-\frac{1}{2}} \\
& \times e^{-\frac{i}{2} \text{sgn}(\epsilon) \left[k\delta \sum_{r=1}^{j-1} \sin[\theta - (N-r)\gamma] + n_0\delta \right]^2}. \tag{45}
\end{aligned}$$

Combining our results we find

$$\begin{aligned}
\psi(\theta, N) &= \text{sgn}(\epsilon)^{-\frac{N}{2}} e^{-i\frac{N}{2}\beta^2\tau} \\
&\times e^{-ik \cos(\theta) - ik \sum_{j=1}^{N-1} [\cos[\theta - (N-j)\gamma] + \delta^2 \text{sgn}(\epsilon)\beta \sin[\theta - (N-j)\gamma](N-j)]} \\
&\times e^{in_0(\theta - N\gamma - N\delta^2 \text{sgn}(\epsilon)\beta)} \\
&\times \left(\prod_{j=1}^N \left(\text{sgn}(\epsilon) + k\delta^2 \sum_{r=1}^{j-1} \cos[\theta - (N-r)\gamma] \right)^{-\frac{1}{2}} \right) \\
&\times e^{\sum_{j=1}^N \left\{ -\frac{i\delta^2}{2} \text{sgn}(\epsilon) [k \sum_{r=1}^{j-1} \sin[\theta - (N-r)\gamma] + n_0]^2 \right\}}. \tag{46}
\end{aligned}$$

3.3 Validity of the Simplification in the Perturbation Series

As mentioned above, we do a simplification, which is valid for

$$\left(1 + k\delta^2 \sum_{r=1}^{j-1} \cos(\theta - (N-r)\gamma) \right)^{-1} \approx 1, \tag{47}$$

where $\gamma = \pi l(1 + 2\beta)$. But for $l = 1$ this seems not to be valid for $\beta = 0.5$ or very close to that point. The behavior of

$$\begin{aligned}
\sum_{r=1}^{j-1} \cos(\theta - (N-r)\gamma) &= \cos(\theta) \sum_{r=1}^{j-1} \cos((N-r)\gamma) \\
&+ \sin(\theta) \sum_{r=1}^{j-1} \sin((N-r)\gamma). \tag{48}
\end{aligned}$$

is shown in figure 2. For $\beta = 0.5$ the sum term will become dominant and our perturbation series will not be valid any more. This will be investigated below in a less heuristic way. Here and in all following studies we will restrict

to the case $l = 1$. We evaluate the sums to find a more meaningful expression.

$$\sum_{r=1}^{j-1} \cos[(N-r)\gamma] \quad (49)$$

$$= \frac{1}{2} \left(e^{iN\gamma} \sum_{r=1}^{j-1} e^{-ir\gamma} + e^{-iN\gamma} \sum_{r=1}^{j-1} e^{ir\gamma} \right) \quad (50)$$

$$= \frac{1}{2} \left(e^{iN\gamma} \frac{1 - e^{-i\gamma(j-1)}}{e^{i\gamma} - 1} + e^{-iN\gamma} \frac{1 - e^{i\gamma(j-1)}}{e^{-i\gamma} - 1} \right) \quad (51)$$

$$= \frac{\sin(\frac{\gamma}{2}(j-1))}{2 \sin(\frac{\gamma}{2})} \left(e^{i(N\gamma - \gamma\frac{j-1}{2} - \frac{\gamma}{2})} + e^{-i(N\gamma - \gamma\frac{j-1}{2} - \frac{\gamma}{2})} \right) \quad (52)$$

$$= \frac{\sin(\frac{\gamma}{2}(j-1))}{\sin(\frac{\gamma}{2})} \cos\left(\left(N - \frac{j}{2}\right)\gamma\right). \quad (53)$$

Similar calculation gives:

$$\sum_{r=1}^{j-1} \sin[(N-r)\gamma] = \frac{\sin(\frac{\gamma}{2}(j-1))}{\sin(\frac{\gamma}{2})} \sin\left(\left(N - \frac{j}{2}\right)\gamma\right). \quad (54)$$

We identify the problematic term as

$$\frac{1}{\sin(\frac{\gamma}{2})}. \quad (55)$$

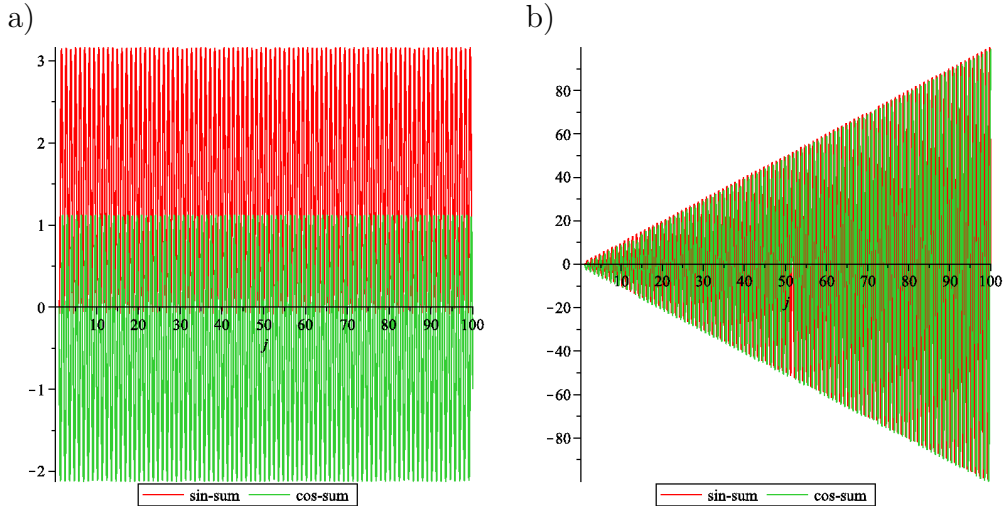


Figure 2: Behavior of the critical sums for $N = 100$, $l = 1$: a) $\beta = 0.4$ b) $\beta = 0.5$.

To fulfill the condition (47) we should at least guarantee

$$\frac{1}{\sin\left(\frac{\gamma}{2}\right)} < \frac{1}{k\delta^2}. \quad (56)$$

Thus we have to restrict the validity of our perturbative result accordingly.

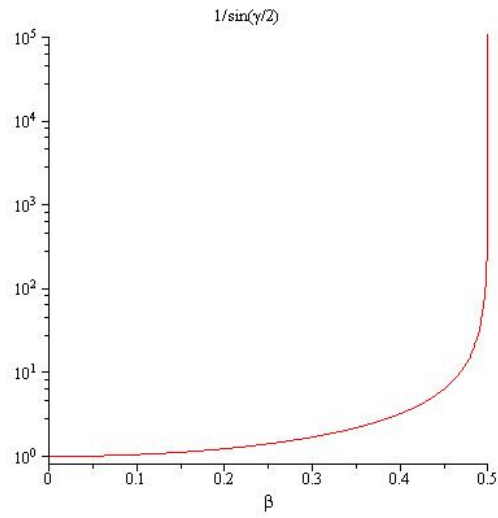


Figure 3: Behavior of the critical term $\frac{1}{\sin\left(\frac{\gamma}{2}\right)}$.

4 Technical Aspects

This section gives a short overview about the techniques we used to calculate numerical reference data and our perturbative results.

4.1 Numerics

To check our perturbative results, we simulate our system numerically. There are two features of the Floquet operator that are fruitful for numerical calculations: first, the Floquet operator factorizes as explained above and second, both the free evolution and the kicking part can be represented by diagonal matrices in the corresponding space. The transition between momentum and θ space can be implemented by a Fast Fourier Transform. As explained in appendix B the FFT-Subroutine will induce the way how we have to translate between the physical meaningful variables θ and n and the corresponding computational vectors. The application flow of the numerical code is sketched in figure 4.

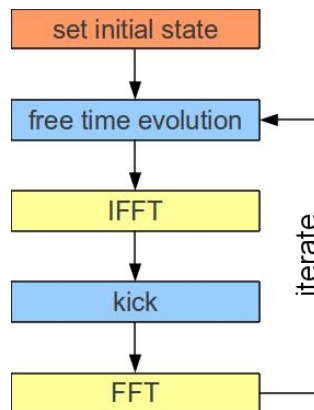


Figure 4: Diagram of numerical calculation.

4.2 Calculation of the Perturbation Series

For the perturbation series we use a FORTRAN code, which calculates $\Psi(\theta_\nu)$ for each θ_ν of our discrete θ space. The formula for the wave function after

N kicks contains the following sums

$$S_1 = \sum_{j=1}^N \cos(\theta - (N - j)\gamma), \quad (57)$$

$$S_2 = \sum_{j=1}^N (N - j) \sin(\theta - (N - j)\gamma), \quad (58)$$

$$IS_1 = \sum_{r=1}^{j-1} \cos(\theta - (N - r)\gamma), \quad (59)$$

$$IS_2 = \sum_{r=1}^{j-1} \sin(\theta - (N - r)\gamma). \quad (60)$$

Using trigonometric addition theorems these can be written as

$$S_1 = \cos(\theta) \sum_{j=1}^N \cos((N - j)\gamma) + \sin(\theta) \sum_{j=1}^N \sin((N - j)\gamma), \quad (61)$$

$$S_2 = \sin(\theta) \sum_{j=1}^N (N - j) \cos((N - j)\gamma) - \cos(\theta) \sum_{j=1}^N (N - j) \sin((N - j)\gamma), \quad (62)$$

$$IS_1 = \cos(\theta) \sum_{r=1}^{j-1} \cos((N - r)\gamma) + \sin(\theta) \sum_{r=1}^{j-1} \sin((N - r)\gamma), \quad (63)$$

$$IS_2 = \sin(\theta) \sum_{r=1}^{j-1} \cos((N - r)\gamma) - \cos(\theta) \sum_{r=1}^{j-1} \sin((N - r)\gamma). \quad (64)$$

This allows to calculate the sums once for a whole θ grid and thus speeds up the calculation. In principle one can evaluate S_1 , IS_1 , IS_2 in the same way as it is done in the investigation of the simplification in the perturbation series, but this would not cause an additional speed up since the number of float point operations will not be decreased.

For our calculations we use one processor of a machine with four QX9650 processors a 3.66GHz and 8GB RAM. The following graph shows the computation time needed for the numerical (black) and perturbation series (red) dependent on the number of kicks for $N_{\text{bas}} = 1024$. The peaks in the curves may correspond to a reduced usage of the processor due to other calculations on the same machine. One should note that for calculations with stepwise

increasing number of kicks N in the numerical calculation one can start from the former wave function while for the perturbation series there is no feature like this. For the dependency of N_{bas} we expect for the numerics $N_{\text{bas}} \log N_{\text{bas}}$, for our perturbation we will have a linear increasing.

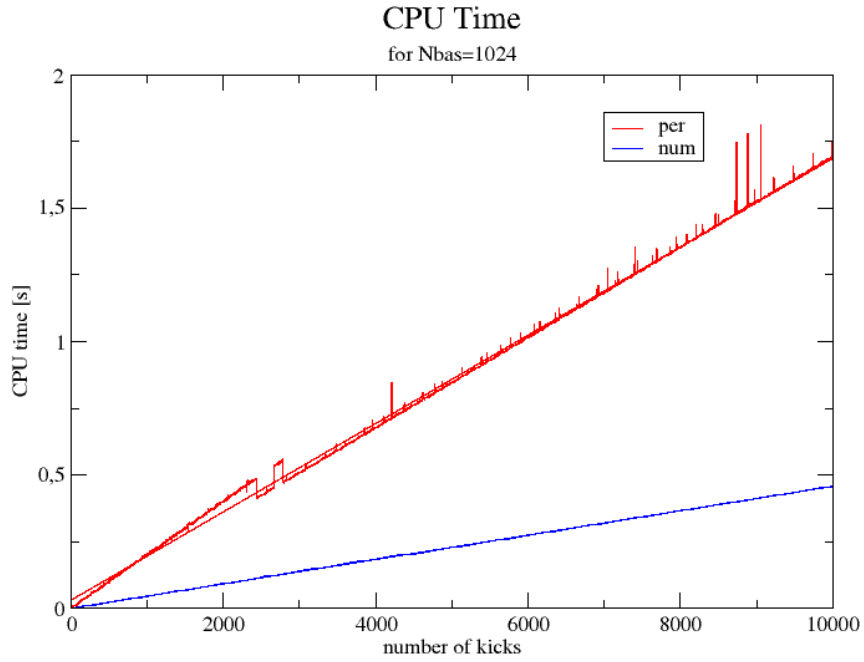


Figure 5: needed CPU time for perturbative (red) and numerical calculation (blue). Fitted slopes: numerics: $4.575 \cdot 10^{-5}$, perturbation: $1.657 \cdot 10^{-2}$.

5 Investigation of the Perturbation Series

A perturbation series is more or less useless if one does not know its range of validity. Therefore we present after a presentation of first results the criterion we use to quantify how good the perturbative calculations are for plane waves and our results. We treat the case of an initial Gaussian in momentum space and finally check the use of our result for studies of fidelity.

5.1 Results

First simulations show that for small δ (recall: $|\epsilon| = \delta^2$) the perturbation is quite good for several hundreds of kicks. But for larger δ it is dramatically worse. This will be studied in a more sophisticated way in the following subsection.

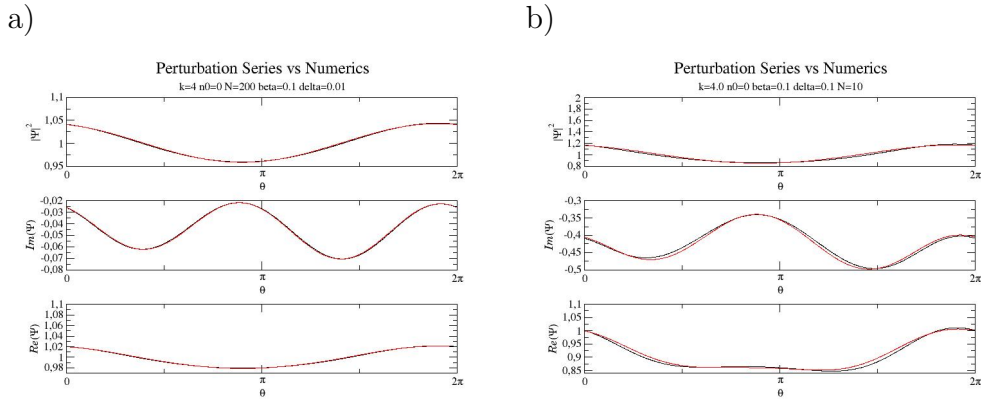


Figure 6: Comparison between the numerically computed wave function (red) in θ space and the one obtained with the perturbative approach for $k = 4$, $n_0 = 0$, $\beta = 0.1$. a) $N = 200$, $\delta = 0.01$ b) $N = 10$, $\delta = 0.1$.

5.2 Time of Validity

To quantify the deviation between numerical and perturbative calculation we use the overlap function

$$o(N) = \frac{\sum_{j=1}^{N_{\text{bas}}} \Psi_{\text{num}}^*(\theta_j, N) \Psi_{\text{per}}(\theta_j, N)}{\sum_{j=1}^{N_{\text{bas}}} \Psi_{\text{num}}^*(\theta_j, N) \Psi_{\text{num}}(\theta_j, N)}. \quad (65)$$

We say the perturbation is okay for

$$|o(N) - 1| < 0.1. \quad (66)$$

The value on the RHS is chosen, such that there is a visible but not too large deviation.

The following two graphs show one example when the deviation reaches the criterion. The second plot shows the wave function in momentum space.

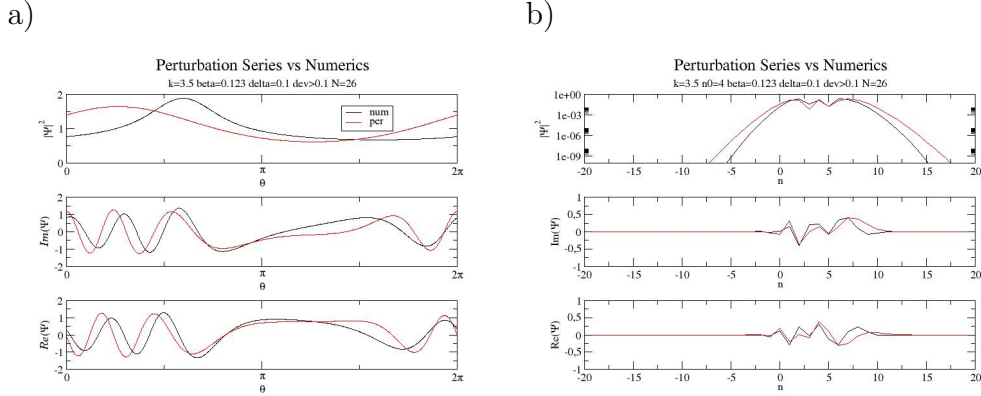


Figure 7: Comparison between perturbative (red) and numerical (black) wave function when the deviation reaches the criterion in θ space (a) and momentum space (b) for $k = 3.5$, $n_0 = 4$, $\beta = 0.123$, $\delta = 0.1$.

In θ space we have visible deviations between numerics and perturbation, but real and imaginary part are still similar. In the modulus squared in momentum space one can recognize in both curves the initial momentum quite easily, but the spreading in the perturbative approach is larger.

Using this criterion we calculated it on the following grid of parameters:

$$k \in [0.25, 4.5] \quad (67)$$

$$\beta \in [0.001, 0.5] \quad (68)$$

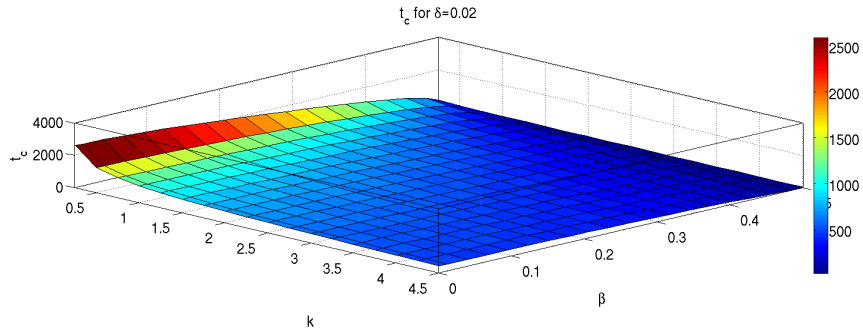
$$\delta \in [0.02, 0.2] \quad (69)$$

The structure of the t_c -surface seems quite similar for different δ , only the scale varies. To the data we fitted the function

$$t_c = a_0 + a_1 \delta^{a_2} \quad (70)$$

We found that $a_2 \approx -2$, for β not close to 0.5. a_0 , a_1 are functions of k and β . Governed by this result, we fixed the exponent of δ to -2 and only fit with the two parameters a_1 and a_0 , where our main interest is in a_1 . The result for a_1 is shown in figure 9. a_0 was always of order one. As one naively would

a)



b)

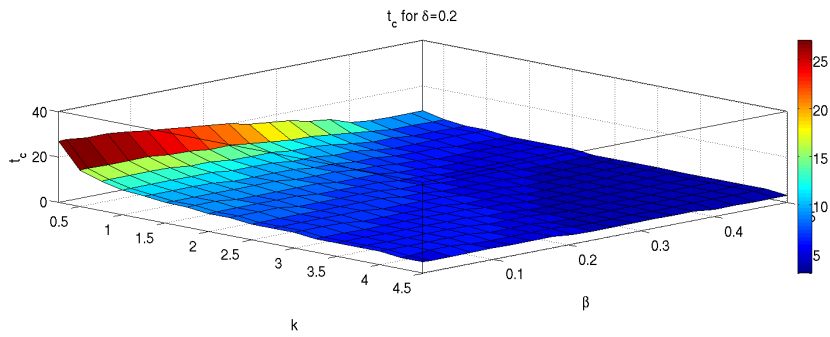


Figure 8: t_c -surfaces for different δ : a) $\delta = 0.02$, b) $\delta = 0.2$.

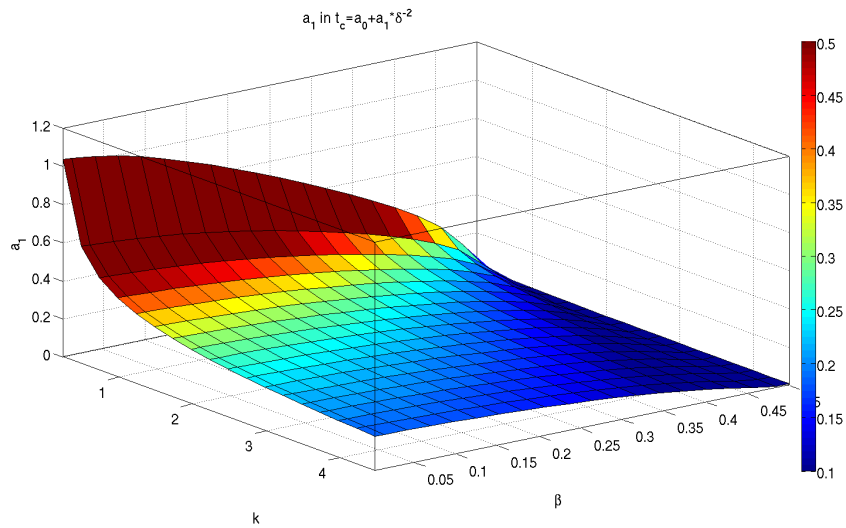


Figure 9: a_1 -surface. The color scale is adjusted such that the behavior in the middle of the plane is visible.

expect, the approximation is better for small k , since here the influence of the kick is not too large. In addition we recognize, that a_1 decreases if one gets close to the resonant value of β , where our perturbation loses validity. Further we checked the dependency on the sign of ϵ and found that there is no significant difference in the development of the overlap for negative ϵ with respect to positive ones.

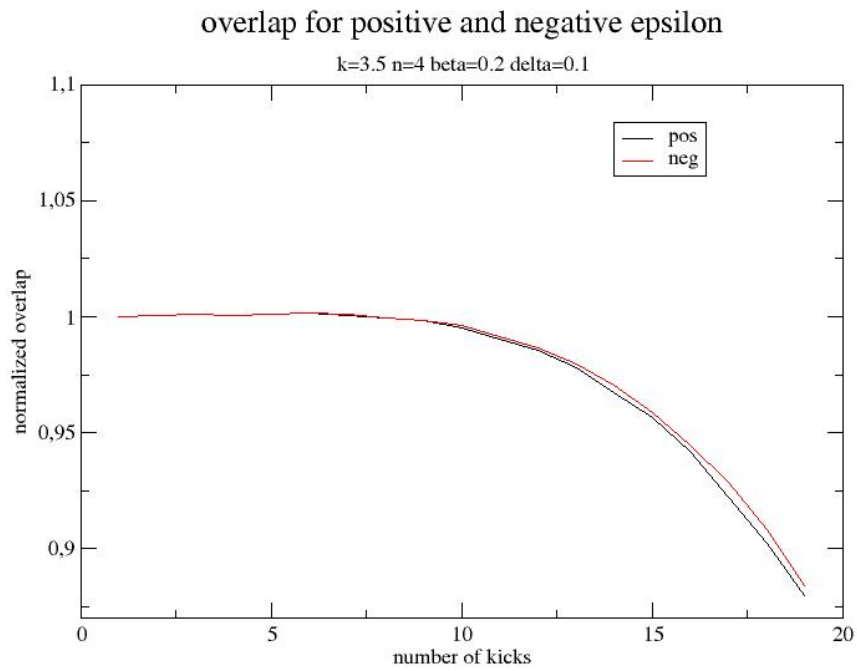


Figure 10: Evolution of the overlap for positive and negative ϵ .

5.3 Initial Gaussian State in Momentum Space

So far we treated only initial δ -peaks in momentum space. In the following subsection we will apply our formalism to initial Gaussian states in momentum space. These states are interesting since they are coherent states in one particle quantum dynamics. Transforming between momentum and position conserves the shape of these states and they have minimal uncertainty.

We start from the initial state

$$\tilde{\Psi}(n, 0) = \frac{e^{-\frac{(n-n_0)^2}{4\sigma^2}}}{(2\pi\sigma^2)^{-\frac{1}{4}}} \quad (71)$$

in momentum space. In θ space this reads

$$\Psi(\theta, 0) = \sum_{m \in \mathbf{Z}} e^{im\theta} \tilde{\Psi}(m, 0) \quad (72)$$

$$= \sum_{m \in \mathbf{Z}} \frac{e^{-\frac{(m-n_0)^2}{4\sigma^2}}}{(2\pi\sigma^2)^{-\frac{1}{4}}} e^{im\theta}. \quad (73)$$

So the wave function is a superposition of plane waves. For each of them, one repeats what was done before. The propagated wave function is a weighted sum of such results.

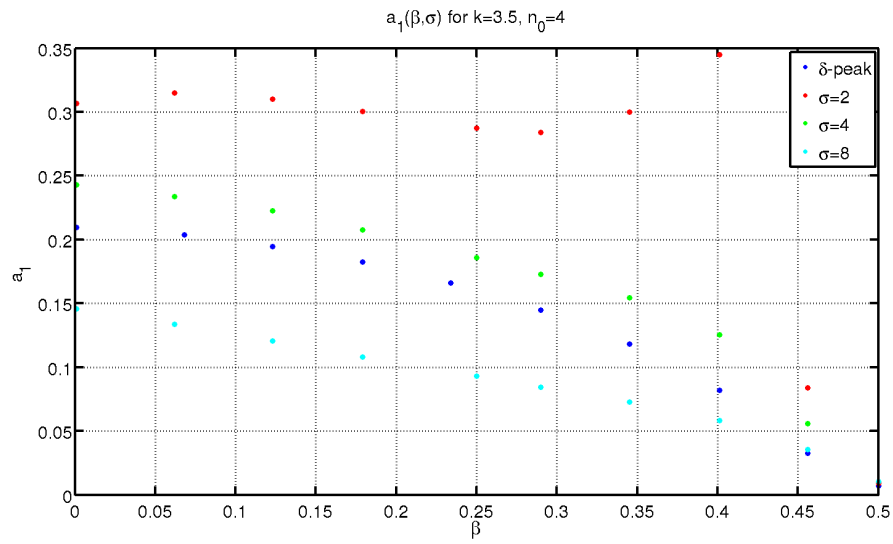
$$\Psi_{\text{co}}(\theta, N) = \sum_m c_m \Psi_m(\theta, N), \quad (74)$$

where Ψ_m is the perturbatively time evolved plane wave with momentum m . For our calculations we restrict to

$$|m - n_0| < 5\sigma. \quad (75)$$

The behavior of a_1 for these initial states is illustrated in figure 11. a_1 becomes larger for $\sigma = 2$ in comparison to the plane wave, which can be understood as an annihilation of errors of the contributing plane waves. This effect vanishes for larger σ . The strange structure for $\sigma = 2$ for large β may arise from the loss of validity for these β .

a)



b)

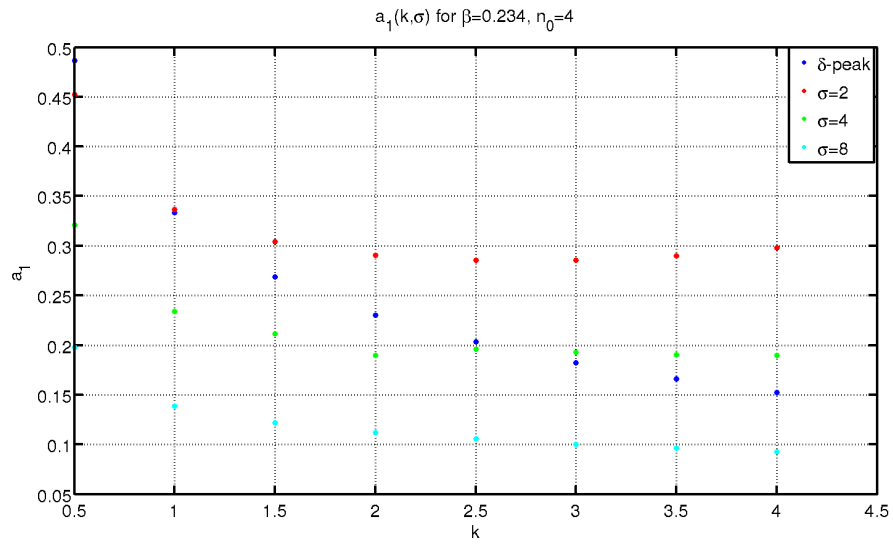


Figure 11: a_1 for initial Gaussian states. a) $a_1(\beta, \sigma)$ b) $a_1(k, \sigma)$.

5.4 Fidelity

Fidelity is defined as the overlap of two wave functions that develop under slightly different dynamics. It is a common measure of stability in quantum mechanics or quantum information [14]. In our case this slightly different dynamics means slightly different k . We will use a normalized version of fidelity

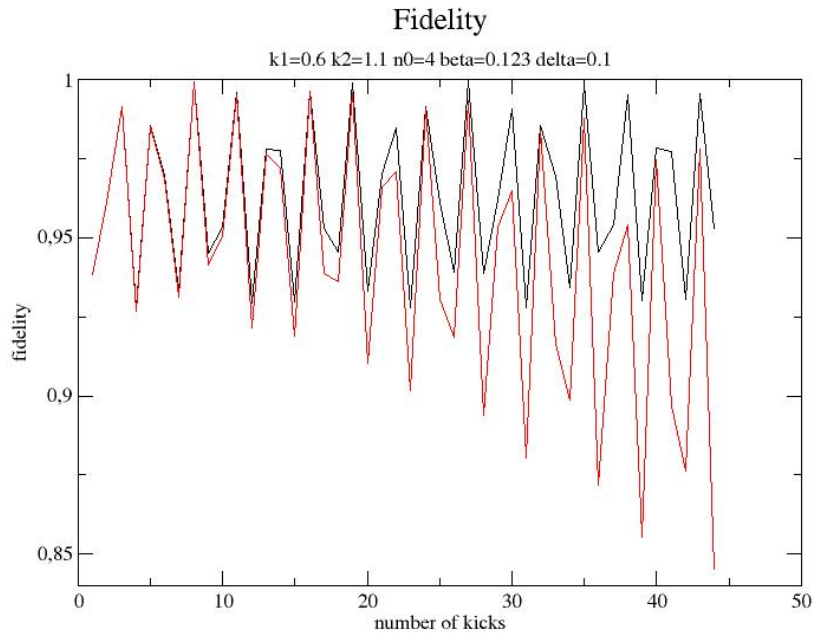
$$f(N) = \frac{|\sum_j \Psi_{k1}^*(\theta_j, N) \Psi_{k2}(\theta_j, N)|}{\sqrt{\sum_j |\Psi_{k1}(\theta_j, N)|^2 \sum_j |\Psi_{k2}(\theta_j, N)|^2}}. \quad (76)$$

As criterion for being off we now use the normalized difference of fidelity:

$$\frac{|f_{\text{num}} - f_{\text{per}}|}{f_{\text{num}}} > 0.1 \quad (77)$$

These results show that unfortunately the deviation between numerical and perturbative wave function dominates. This implies that further studies of fidelity using our perturbative result are meaningful just for very small perturbation parameters, i.e. $|\epsilon| \rightarrow 0$.

a)



b)

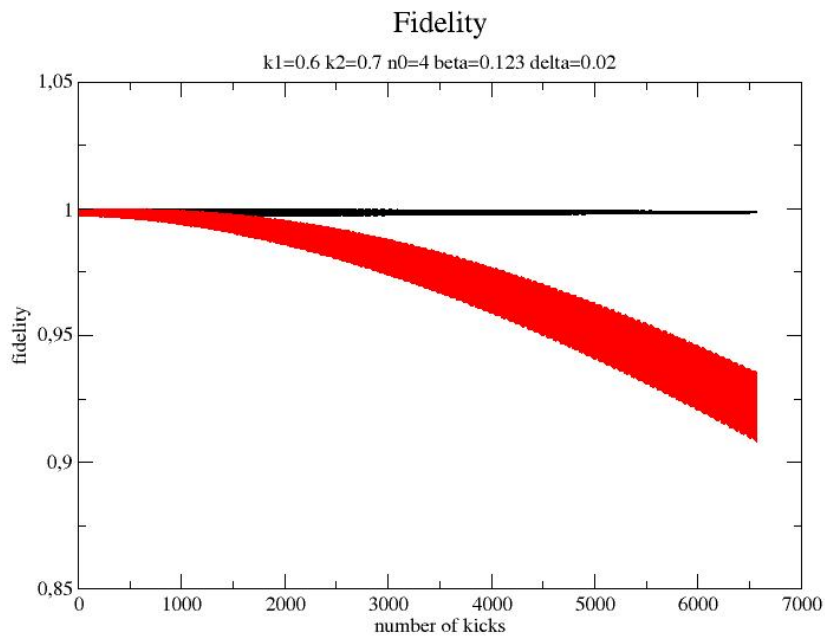


Figure 12: Comparison between perturbative (red) and numerical (black) results of fidelity calculations for different sets of parameters.

6 2D Kicked Rotor

In order to mimic higher dimensional systems one can look at modified versions of the normal kicked rotor [15], where one for example replaces the former time independent kicking strength by a periodic one [16]. This leads to two periodicities in time: first the kicking period T_1 and second the period of the kicking strength T_2 . The Hamiltonian we use reads:

$$H = \frac{p^2}{2} + k(1 + \cos(2\pi \frac{t}{T_2})) \cos(\theta) \sum_{\nu \in \mathbb{Z}} \delta(t - \nu T_1), \quad (78)$$

where p is the momentum, k the kicking strength and θ the angle on the ring. To make this Hamiltonian periodic in time we have to choose T_1 and T_2 commensurable. In the following we will restrict ourselves to the case $T_2 = qT_1$ with integer q .

6.1 Classical Description

This Hamiltonian leads to a map that can be treated as a sequence of q normal kicked rotor maps, but with the important change of a now time dependent kicking strength:

$$\begin{pmatrix} \theta_{n+1} \\ p_{n+1} \end{pmatrix} = \Phi \begin{pmatrix} \theta_n \\ p_n \end{pmatrix}, \quad (79)$$

$$\Phi = \phi_q \circ \phi_{q-1} \circ \dots \circ \phi_1, \quad (80)$$

where ϕ_m is given by

$$\phi_m : \begin{pmatrix} \theta_m \\ p_m \end{pmatrix} \rightarrow \begin{pmatrix} \theta_m + p_m T_1 \\ p_m + k_m \sin(\theta_{m+1}) \end{pmatrix} \quad (81)$$

and

$$k_m = k \left(1 + \cos(2\pi \frac{m}{q}) \right). \quad (82)$$

In the same way as for the kicked rotor this map is 2π periodic in θ and p .

6.2 Quantum Mechanical and ϵ -classical Description

Since the Hamiltonian is periodic in time one can write down a Floquet operator. Similar to the classical description it can be built up of blocks corresponding to the normal kicked rotor:

$$U = \mathcal{T} \prod_{m=1}^q \left[e^{-ik_m \cos(\hat{\theta})} e^{-i\frac{t}{2}\tau} \right] \quad (83)$$

Again we have quantum resonances for $\tau = 4\pi j$ with integer j . In the following we will only treat the case $\tau = 4\pi$. In analogy to the studies of the Quantum Kicked Rotor we will use ϵ -classics to study the system close to resonance. We find the effective Hamiltonian

$$\tilde{H} = \frac{I^2}{2\text{sgn}(\epsilon)} + k|\epsilon|(1 + \cos(2\pi\frac{t}{T_2})) \cos(\theta) \sum_{\nu \in \mathbb{Z}} \delta(t - \nu T_1). \quad (84)$$

This leads to the map:

$$\Phi = \phi_q \circ \phi_{q-1} \circ \dots \circ \phi_1, \quad (85)$$

where

$$\phi_m : \begin{pmatrix} \theta_m \\ I_m \end{pmatrix} \rightarrow \begin{pmatrix} \theta_m + \text{sgn}(\epsilon)I_m \\ I_m + k_m|\epsilon| \sin(\theta_{m+1}) \end{pmatrix} \quad (86)$$

and

$$k_m = k \left(1 + \cos(2\pi\frac{m}{q}) \right). \quad (87)$$

In the same way as in the kicked rotor the important quantity beside the periods is $k|\epsilon|$.

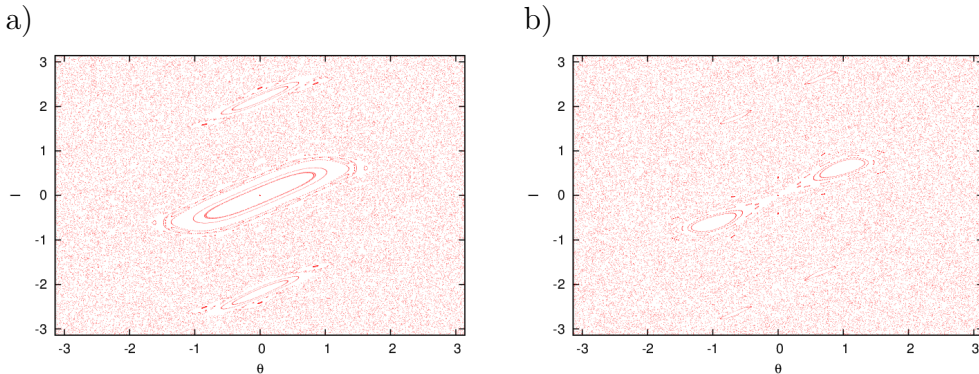


Figure 13: ϵ -classical phase space for $q = 3$ and different $k|\epsilon|$. a) $k|\epsilon| = 0.613$ b) $k|\epsilon| = 0.746$. In both plots we started from a grid of 100 points over the whole phase space and applied Φ 200 times.

6.3 Fixed Points

The phase space shown in figure 13a shows three islands of stability surrounded by a chaotic sea. As usual in the center of each of them there is a

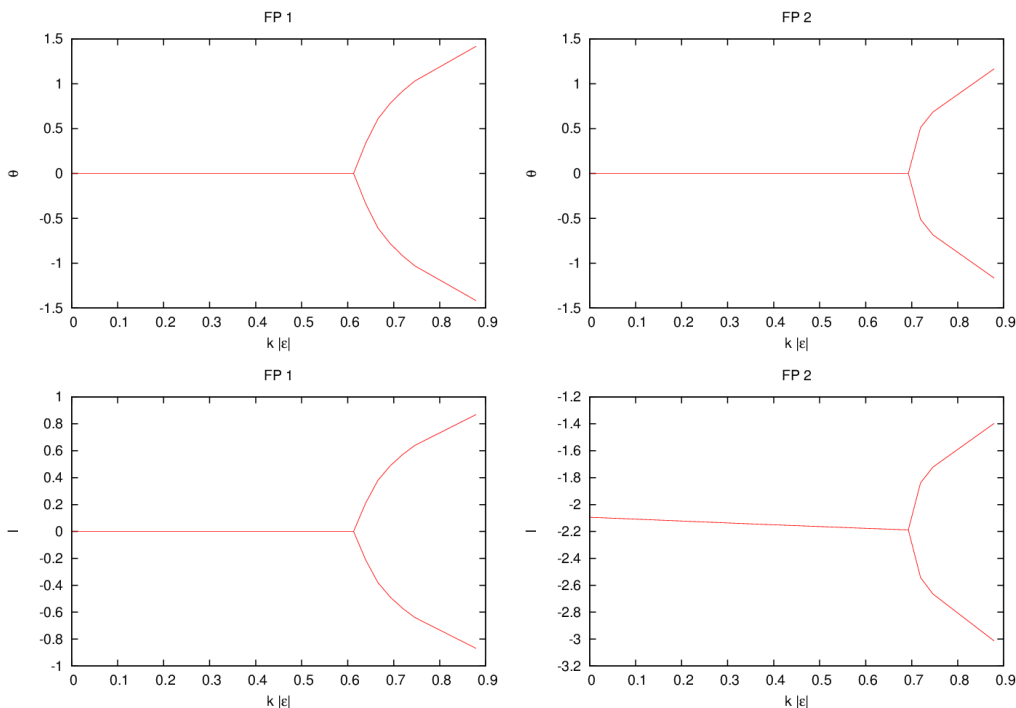


Figure 14: Position (θ, I) of the fixed points in dependency of $k|\epsilon|$.

stable fixed point. Since the chaotic behavior is dominated by $k|\epsilon|$, we study the development of the fixed points in dependency of this quantity.

While the fixed point at $(0, 0)$ can be seen immediately from the map, the others have to be calculated numerically. Since the mapping is point symmetric to $(0, 0)$ we can restrict our studies to one of them. As shown in 14 the central island is less stable than the outer ones.

To treat the stability of the non traveling fixed point at $(0, 0)$ in a more sophisticated way we linearized the map around this point and check the stability via the criterion [17]

$$|\text{tr}(M')| < 2, \quad (88)$$

where M' is the linearized map around the fixed points. The point when the central island becomes unstable that can be seen in figure 15 coincides with the point when we see this instability in the phase space plots. Another question one can ask is where are the outer islands with $\theta = 0$ for $k|\epsilon| \rightarrow 0$ and can we understand their occurrence. To answer this question we will give a heuristic argument: Lets consider the case $k|\epsilon| = 0$ and for simplicity we fix $\text{sgn}(\epsilon) = 1$. The map Φ becomes the composition of q equal maps ϕ

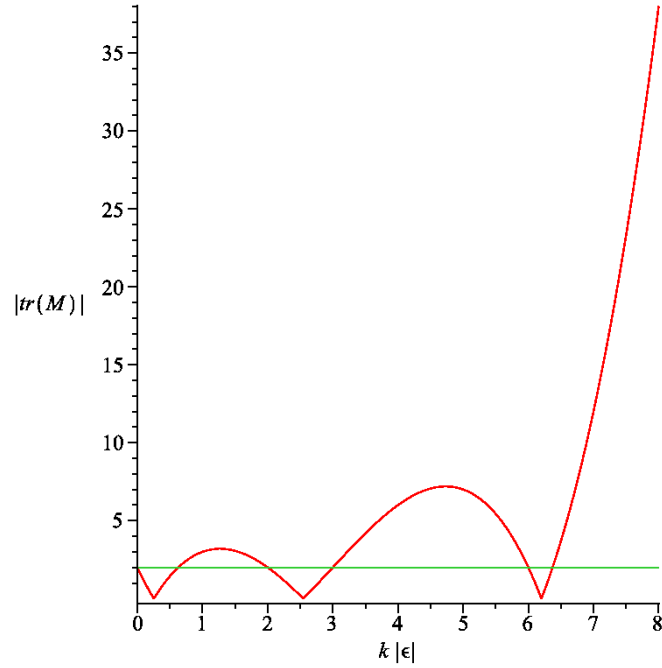


Figure 15: Stability analysis of the fixed point $(0,0)$ for $q = 3$. The fixed point is stable if $|\text{tr}(M)|$ (red) is less than 2 (green line).

and one gets:

$$\Phi : \begin{pmatrix} \theta \\ I \end{pmatrix} \rightarrow \begin{pmatrix} \theta + qI \\ I \end{pmatrix}. \quad (89)$$

We are interested in $2\pi n = qI$ with integer n . Since we are periodic in I as well we find q different values for I .

Expansion of the initial map in $k|\epsilon|$ for an certain value of q gives the same result. This argument shows that the number of islands for small $k|\epsilon|$ arises from the composition of single kicked rotor maps and their periodicity.

7 Conclusion and Outlook

In the thesis we built an perturbation series for the Quantum Kicked Rotor close to quantum resonance. Unfortunately we found that the range of our perturbation series up to second order in $\delta = \sqrt{|\epsilon|}$ is restricted to very small detunings from resonance ϵ . Further it loses its validity if one takes a quasi-momentum very close to the resonant value. But for this case there exists a working pendulum approximation [18, 19]. At least at this point we see no simple way to go to higher orders in the perturbation series since we expect folded multi-dimensional integrals which can not be solved analytically. Nevertheless we have a perturbation theory for very small $|\epsilon|$ or for a small number of kicks for which we can give the range of validity. One possible extension could be the accelerated Quantum Kicked Rotor, where one deals with an additional acceleration of the particle on the line [7].

The Quantum Kicked Rotor with a periodic change of the kicking strength could be studied for the case of commensurable and incommensurable frequencies starting from an ϵ -classical point of view. Moreover one can ask the question how energy grows in this system. In particular what is the diffusion constant, what is the break time for Dynamical Localization? Another question might be the stability of quantum resonances if one treats the system with noise as it has been done for example in the standard Quantum Kicked Rotor [20, 21].

A The Quantum Propagator - Some Examples

In this Appendix we will study some simple examples for the propagator formalism starting from the well-known propagator of a free particle [11, 12]

$$K_f(x, t|x_0, 0) = \left(\frac{m}{2\pi i\hbar t}\right)^{\frac{1}{2}} \exp\left(\frac{im(x-x_0)^2}{2\hbar t}\right). \quad (90)$$

Some of the following examples can be found in textbooks like [11, 12].

A.1 Bouncing Particle Between Two Walls

We consider the potential [22]

$$V(x) = \begin{cases} 0 & 0 < x < a \\ \infty & \text{otherwise} \end{cases} \quad (91)$$

and the initial state

$$\psi_0(x) = \delta(x - x_0), \quad (92)$$

where $0 < x_0 < a$.

For simplicity we will first study the simpler case of only one wall at $x = 0$. The free propagator $K_f(x, t|x_0, 0)$ includes all possible paths starting from x_0 ending at x . But in our problem paths that cross the wall are not allowed. These paths can be taken equivalent to paths starting from $-x_0$ ending at x , since a path from x_0 to the point of last crossing the wall can be mirrored at the wall. Thus we find the propagator for the problem with one wall

$$K(x, t|x_0, 0) = K_f(x, t|x_0, 0) - K_f(x, t|-x_0, 0). \quad (93)$$

The situation with two walls is a little bit more complicated. Now both walls can be treated as mirrors and thus we get an infinite number of boxes on the x -axis $[ja, (j+1)a]$ with $j \in \mathbb{Z}$, where each wall acts as a mirror plane between neighboring boxes. For the mirror sources we get

$$x_j = \begin{cases} j \cdot a + x_0 & , j \text{ even} \\ (j+1) \cdot a - x_0 & , j \text{ odd} \end{cases}. \quad (94)$$

Paths crossing an odd number of walls are not allowed, while those crossing an even number are allowed. The latter correspond to paths with reflections. For the path crossing one wall we subtract $K_f(x, t|x_1, 0)$ and $K_f(x, t|-x_1, 0)$,

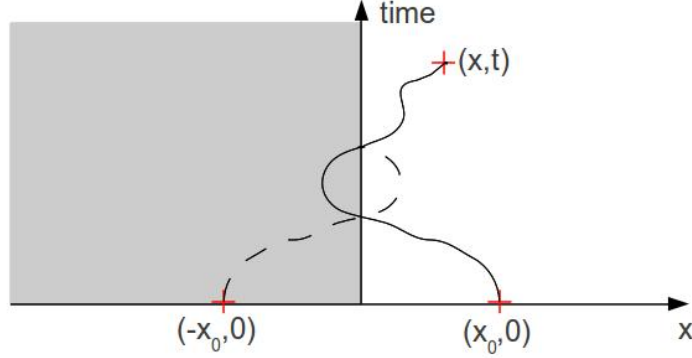


Figure 16: Particle in front of a wall.

but this excludes allowed paths crossing two walls. Therefore we have to add $K_f(x, t|x_2, 0)$ and $K_f(x, t|-x_2, 0)$. Thereafter we must subtract $K_f(x, t|x_3, 0)$ and $K_f(x, t|-x_3, 0)$ and so on. Thus we get

$$K(x, t|x_0, 0) = \sum_{j \in \mathbb{Z}} (-1)^j K_f(x, t|x_j, 0). \quad (95)$$

Or inserting x_j and after some shifting of indices

$$K(x, t|x_0, 0) = \sum_{j \in \mathbb{Z}} (K_f(x, t|2ja + x_0, 0) - K_f(x, t|2ja - x_0, 0)). \quad (96)$$

A.2 Particle on a Ring

Next we are interested in a free particle on a ring [23]. The Hamiltonian is

$$H = \frac{p^2}{2m} = -\frac{1}{2mR^2} \frac{d^2}{d\theta^2}. \quad (97)$$

In general the initial state after a time t is given by

$$\psi(x, t) = \int dx_0 K(x, t|x_0, 0) \psi(x_0, 0). \quad (98)$$

In our case we have due to the periodicity of the position coordinate

$$\psi(\theta, t) = \int_0^{2\pi} d\theta_0 K(\theta, t|\theta_0, 0) \psi(\theta_0, 0), \quad (99)$$

where the factor R from the measure is absorbed in the propagator. Due to the periodic boundary conditions we have to take not only paths from θ_0 to

θ but also paths starting from $\theta_0 + 2\pi j$, where $j \in \mathbb{Z}$, into account. Thus we finally have:

$$K(\theta, t|\theta_0, 0) = \sum_{j \in \mathbb{Z}} R \left(\frac{m}{2\pi i \hbar t} \right)^{\frac{1}{2}} \exp \left(\frac{imR^2(\theta - \theta_0 - 2\pi j)^2}{2\hbar t} \right) \quad (100)$$

Using Poisson's formula [24]

$$\sum_{j \in \mathbb{Z}} f(j) = \sum_{J \in \mathbb{Z}} \int_{-\infty}^{\infty} f(x') e^{-2\pi i J x'} dx' \quad (101)$$

one can show that this is equal to the result we would get by expressing the propagator via expanding the initial state in energy eigenstates $|k\rangle$ and using the time evolution operator $\hat{U}_t = e^{-\frac{i}{\hbar} \int_0^t \hat{H} d\tau}$. In our case these eigenstates are plane waves $\frac{1}{\sqrt{2\pi}} e^{-ik\theta}$, which yields

$$K(\theta, t|\theta_0, 0) = \sum_{k \in \mathbb{Z}} \langle \theta | k \rangle \exp \left(\frac{i}{\hbar} E_k t \right) \langle k | \theta_0 \rangle = \sum_k e^{-ik(\theta - \theta_0)} e^{-\frac{i\hbar k^2 t}{2mR^2}}. \quad (102)$$

A.3 Shifted Momentum

We now treat the case of shifted momentum

$$H = \frac{(p + p_0)^2}{2m}. \quad (103)$$

Since the propagator can be regarded as transition amplitude, we can write:

$$K(x_f, t|x_0, 0) \quad (104)$$

$$= \langle x_f, t|x_0, 0 \rangle = \langle x_f, t|e^{-\frac{i}{\hbar} \int_0^t \hat{H}(t') dt'}|x_0, 0 \rangle \quad (105)$$

$$= \int \int dp dp' \langle x_f, t|p \rangle \langle p|e^{-\frac{i}{\hbar} \frac{(p+p_0)^2}{2m} t}|p' \rangle \langle p'|x_0, 0 \rangle \quad (106)$$

$$= \int dp \langle x_f, t|p \rangle e^{-\frac{i}{\hbar} \frac{(p+p_0)^2}{2m} t} \langle p|x_0, t \rangle \quad (107)$$

$$= \frac{1}{2\pi\hbar} \int dp e^{\frac{i}{\hbar} p(x_f - x_0)} e^{-\frac{i}{\hbar} \frac{(p+p_0)^2}{2m} t} \quad (108)$$

$$= \frac{1}{2\pi\hbar} \int dp e^{-\frac{it}{2m\hbar} (p^2 - 2p(\frac{m}{t}(x_f - x_0) - p_0) + p_0^2)} \quad (109)$$

$$= \frac{1}{2\pi\hbar} \int dp e^{-\frac{it}{2m\hbar} (p - (\frac{m}{t}(x_f - x_0) - p_0))^2} e^{-\frac{it}{2m\hbar} p_0^2} e^{\frac{it}{2m} (\frac{m}{t}(x_f - x_0) - p_0)^2} \quad (110)$$

$$= \frac{1}{2\pi\hbar} \sqrt{\frac{2\pi\hbar m}{it}} e^{-\frac{it}{2m\hbar} p_0^2} e^{\frac{it}{2m} (\frac{m}{t}(x_f - x_0) - p_0)^2} \quad (111)$$

$$= \left(\frac{m}{2\pi i \hbar t} \right)^{\frac{1}{2}} e^{-\frac{it}{2m\hbar} p_0^2} e^{\frac{it}{2m} (\frac{m}{t}(x_f - x_0) - p_0)^2}. \quad (112)$$

A.4 Initial Velocity

Starting from the Lagrangian

$$\mathcal{L} = \frac{m}{2}(v + v_0)^2 \quad (113)$$

we get the canonical momentum $p = m(v + v_0)$ and the Hamiltonian

$$H = pv - \mathcal{L} \quad (114)$$

$$= \frac{p^2}{2m} + pv_0. \quad (115)$$

We find

$$K(x_f, t|x_0, 0) \quad (116)$$

$$= \langle x_f, t|x_0, 0 \rangle = \langle x_f, t|e^{-\frac{i}{\hbar} \int_0^t \hat{H}(t') dt}|x_0, 0 \rangle \quad (117)$$

$$= \int \int dp dp' \langle x_f, t|p \rangle \langle p|e^{-\frac{i}{\hbar} \left(\frac{p^2}{2m} + \hat{p}v_0 \right) t}|p' \rangle \langle p'|x_0, 0 \rangle \quad (118)$$

$$= \int dp \langle x_f, t|p \rangle e^{-\frac{i}{\hbar} \left(\frac{p^2}{2m} + pv_0 \right) t} \langle p|x_0, 0 \rangle \quad (119)$$

$$= \frac{1}{2\pi\hbar} \int dp e^{\frac{i}{\hbar} p(x_f - x_0)} e^{-\frac{i}{\hbar} \left(\frac{p^2}{2m} + \hat{p}v_0 \right) t} \quad (120)$$

$$= \frac{1}{2\pi\hbar} \int dp e^{-\frac{it}{2m\hbar} [p^2 + 2p(mv_0 - \frac{m}{t}(x_f - x_0))]} \quad (121)$$

$$= \frac{1}{2\pi\hbar} \int dp e^{-\frac{it}{2m\hbar} [p + (mv_0 - \frac{m}{t}(x_f - x_0))]^2} e^{\frac{imt}{2\hbar} (v_0 - \frac{x_0 - x_f}{t})^2} \quad (122)$$

$$= \frac{1}{2\pi\hbar} \sqrt{\frac{2\pi\hbar m}{it}} e^{\frac{imt}{2\hbar} (v_0 - \frac{x_f - x_0}{t})^2} \quad (123)$$

$$= \left(\frac{m}{2\pi i \hbar t} \right)^{\frac{1}{2}} e^{\frac{imt}{2\hbar} (v_0 - \frac{x_f - x_0}{t})^2}. \quad (124)$$

Another way to solve this problem is to start from (103) and gauge the term $\frac{p_0}{2m}$ away. This leads to a gauge factor of

$$e^{i \frac{t}{\hbar} \frac{p_0^2}{2m}}. \quad (125)$$

A.5 Time Evolution of a Particle in the 1-dim Harmonic Oscillator

Starting from the harmonic oscillator Hamiltonian

$$H = \frac{p^2}{2m} + \frac{m\omega^2}{2} x^2 \quad (126)$$

we want to study the time evolution of an initial Gaussian wave packet centered at x_0

$$\psi(x_i, 0) = (2\pi\sigma^2)^{-\frac{1}{4}} \exp\left(-\frac{(x_i - x_0)^2}{4\sigma^2}\right). \quad (127)$$

The propagator of the harmonic oscillator is [11]

$$K(x, t|x_i, 0) = \left(\frac{m\omega}{2\pi i\hbar \sin(\omega t)}\right)^{\frac{1}{2}} \exp\left(\frac{im\omega}{2\hbar \sin(\omega t)}[(x^2 + x_i^2) \cos(\omega t) - 2xx_i]\right). \quad (128)$$

The state at time t is given by

$$\psi(x, t) = \int_{-\infty}^{\infty} dx_i K(x, t|x_i, 0) \psi(x_i, 0). \quad (129)$$

After rearranging terms this reads

$$\begin{aligned} \psi(x, t) &= (2\pi\sigma^2)^{-\frac{1}{4}} \left(\frac{m\omega}{2\pi i\hbar \sin(\omega t)}\right)^{\frac{1}{2}} \exp\left(\frac{im\omega \cos(\omega t)x^2}{2\hbar \sin(\omega t)} - \frac{x_0^2}{4\sigma^2}\right) \\ &\times \int_{-\infty}^{\infty} dx_i \exp\left\{-\left(\frac{m\omega \cos(\omega t)}{2\hbar i \sin(\omega t)} + \frac{1}{4\sigma^2}\right)x_i^2 + \left(\frac{m\omega x}{\hbar i \sin(\omega t)} + \frac{x_0}{2\sigma^2}\right)x_i\right\}. \end{aligned} \quad (130)$$

The Gaussian integral can be computed via (44).

$$\begin{aligned} \psi(x, t) &= (2\pi\sigma^2)^{-\frac{1}{4}} \Delta(t)^{-\frac{1}{2}} \exp\left(\frac{im\omega \cos(\omega t)x^2}{2\hbar \sin(\omega t)} - \frac{x_0^2}{4\sigma^2}\right) \\ &\times \exp\left(\frac{1}{2m\omega\sigma^2\Delta(t)} \left(\frac{m^2\omega^2\sigma^2}{i\hbar \sin(\omega t)} + m\omega x x_0 + \frac{\hbar i \sin(\omega t)}{4\sigma^2 x_0^2}\right)\right), \end{aligned} \quad (131)$$

where $\Delta(t) = \cos(\omega t) + \frac{i\hbar \sin(\omega t)}{2m\omega\sigma^2}$. We are interested in $|\psi(x, t)|^2$. Therefore we need the real part of the second exponential term which yields

$$\frac{1}{2m\omega\sigma^2|\Delta(t)|^2} \left(-\frac{m\omega}{2}x^2 + m\omega x x_0 \cos(\omega t) + \frac{\hbar^2 \sin^2(\omega t)}{8m\omega\sigma^4}x_0^2\right). \quad (132)$$

Thus we finally have

$$|\psi(x, t)|^2 = (2\pi\sigma^2|\Delta(t)|^2)^{-\frac{1}{2}} \exp\left(-\frac{(x - x_0 \cos(\omega t))^2}{2\sigma^2|\Delta(t)|^2}\right). \quad (133)$$

In agreement with Ehrenfest's theorem the center of the wave packet oscillates between $-x_0$ and x_0 . The width oscillates with the same frequency ω . In the limit $\omega = 0$ we find the behavior of a free Gaussian wave packet

$$|\psi(x, t)|^2 = \left(2\pi\sigma^2 \left(1 + \frac{\hbar^2 t^2}{4m^2\sigma^4}\right)\right)^{-\frac{1}{2}} \exp\left(-\frac{(x - x_0)^2}{2\sigma^2 \left(1 + \frac{\hbar^2 t^2}{4m^2\sigma^4}\right)}\right). \quad (134)$$

B FFT Subroutine

In the numerical simulation we use a subroutine performing a discrete Fourier transform between our computational variables x and p .

$$x = 1, \dots, N_{bas} \quad (135)$$

$$p = 1, \dots, N_{bas}, \quad (136)$$

where N_{bas} is the length of our basis. A common way to define a discrete Fourier transform is:

$$\tilde{\Psi}_p = \mathcal{F}[\Psi] = \sum_{x=1}^{N_{bas}} e^{-i \frac{2\pi}{N_{bas}} (p-1)(x-1)} \Psi_x \quad (137)$$

$$\Psi_x = \mathcal{F}^{-1}[\tilde{\Psi}] = \frac{1}{N_{bas}} \sum_{p=1}^{N_{bas}} e^{i \frac{2\pi}{N_{bas}} (p-1)(x-1)} \tilde{\Psi}_p. \quad (138)$$

To find what the subroutine does, we tested it with δ -peaks and Gaussian wave packets. We found:

$$\tilde{\Psi}_p = \mathcal{S}_{isn=-1}[\Psi] = \sum_{x=1}^{N_{bas}} e^{-i \frac{2\pi}{N_{bas}} (p-1)(x-1)} \Psi_x \quad (139)$$

$$\Psi_x = \mathcal{S}_{isn=1}[\tilde{\Psi}] = \sum_{p=1}^{N_{bas}} e^{i \frac{2\pi}{N_{bas}} (p-1)(x-1)} \tilde{\Psi}_p, \quad (140)$$

where isn is a parameter which is needed, if one calls the subroutine. This parameter sets the sign in the exponential. Further one has to take care of the missing normalization factor $\frac{1}{N_{bas}}$, which must be included by hand. An other point of interest is the transition between the computational variables x and p and the physical variables $\theta \in [0, 2\pi)$ and $n \in \mathbf{Z}$. This transition is induced by the FFT subroutine as follows:

$$x = \frac{\theta_x}{2\pi} N_{bas} + 1 \quad (141)$$

$$p = \begin{cases} n + 1 & n \geq 0 \\ N_{bas} + 1 - |n| & n < 0 \end{cases}. \quad (142)$$

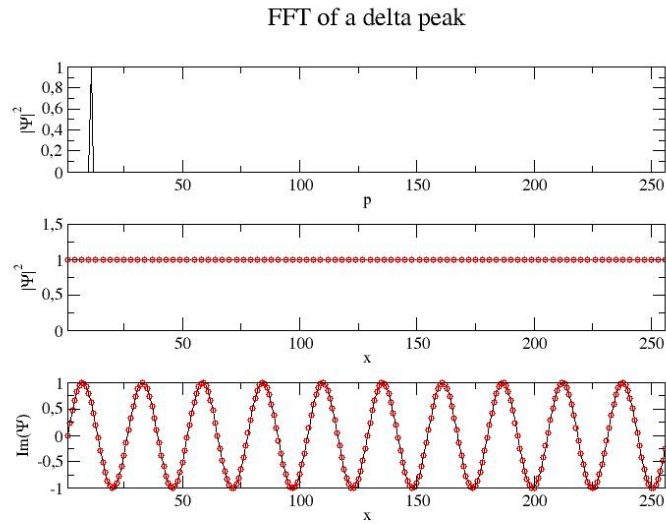


Figure 17: Inverse FFT of $\Psi_p = \delta_{p,11}$. black: subroutine, red: formula applied by Maple.

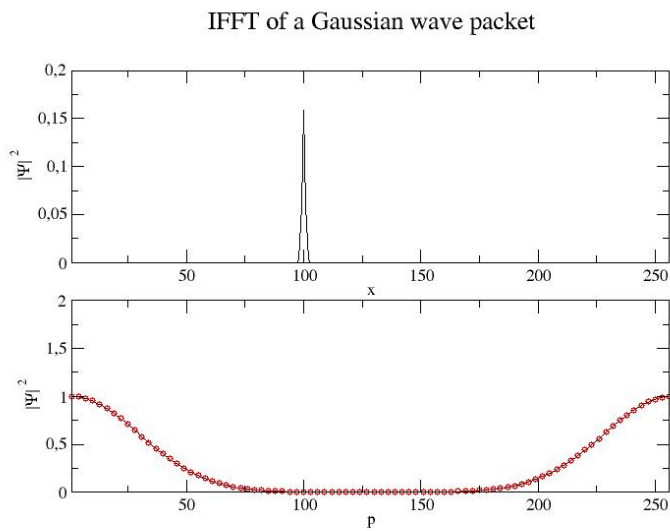


Figure 18: FFT of $\Psi_x = \frac{e^{-\frac{(x-100)^2}{2}}}{\sqrt{2\pi}}$. black: subroutine, red: formula applied by Maple.

The transition $p \leftrightarrow n$ becomes clear, if one looks at the Fourier transform of a Gaussian wave packet (fig. 18), where a Gaussian in n is expected. Figure 19 may clarify the transition.

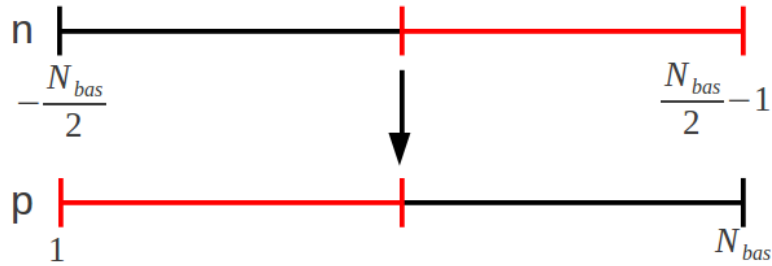


Figure 19: Transition between n and p .

The factor $(x - 1)$ in $x \leftrightarrow p$ transition could be verified by looking at the data files of the inverse Fourier transform of a δ -peak, where $x = 1$ equaled $\theta = 0$.

Bibliography

- [1] B. V. Chirikov, Phys. Rep. **52**, 263 (1979).
- [2] F. M. Izrailev, Phys. Rep. **196**, 299 (1990).
- [3] S. Fishman, D. Grempel, and R. Prange, Phys. Rev. Lett. **49**, 509 (1982).
- [4] M. Raizen, Adv. At. Mol. Phys. **41**, 43 (1999).
- [5] F. Moore, C. Robinson, C. Bharucha, B. Sundaram, and M. Raizen, Phys. Rev. Lett. **75**, 4598 (1995).
- [6] C. Ryu *et al.*, Phys. Rev. Lett. **96**, 160403 (2006).
- [7] S. Fishman, I. Guarneri, and L. Rebuzzini, Journal of Statistical Physics **110**, 911 (2003).
- [8] M. Sadgrove and S. Wimberger, Adv. At. Mol. Opt. Phys. **60**, in print (2011).
- [9] A. Peres, Phys. Rev. A **30**, 1610 (1984).
- [10] R. P. Feynman, Rev. Mod. Phys. **20**, 367 (1948).
- [11] R. P. Feynman and A. R. Hibbs, *Quantum mechanics and path integrals*, 20. [pr.] ed. (McGraw-Hill, New York, 1995).
- [12] H. Kleinert, *Path integrals in quantum mechanics, statistics, polymer physics, and financial markets*, 5. ed. (World Scientific, New Jersey, 2009).
- [13] R. Graham, M. Schlautmann, and P. Zoller, Phys. Rev. A **45**, R19 (1992).
- [14] M. A. Nielsen and I. L. Chuang, *Quantum computation and quantum information*, 10. print. ed. (Cambridge Univ. Press, Cambridge, 2009).
- [15] G. Casati, I. Guarneri, and D. L. Shepelyansky, Phys. Rev. Lett. **62**, 345 (1989).
- [16] D. Shepelyansky, Physica D **28**, 103 (1987).
- [17] A. J. Lichtenberg and M. A. Leiberman, *Regular and chaotic dynamics*, Applied mathematical sciences No. 38, 2. ed. (Springer, 1992).

- [18] B. Probst, *The Pendulum Approximation for Fidelity in Quantum Kicked Rotor Systems*, Master's thesis, University of Heidelberg, 2010.
- [19] M. Abb, *Fidelity for Kicked Atoms at nearly Resonant Driving*, Master's thesis, University of Heidelberg, 2009.
- [20] S. Wimberger, *Chaos and Localisation: Quantum Transport in Periodically Driven Atomic Systems*, PhD thesis, Ludwig-Maximilians-Universität München and Università degli Studi dell' Insubria Como, 2004.
- [21] M. Sadgrove, S. Wimberger, S. Parkins, and R. Leonhardt, Phys. Rev. E **78**, 25206 (2008).
- [22] M. Goodman, Am. J. Phys. **49**, 843 (1981).
- [23] G.-L. Ingold, Path integrals and their application to dissipative quantum systems, in *Coherent Evolution in Noisy Environments*, edited by A. Buchleitner and K. Hornberger, volume 611 of *Lecture Notes in Physics*, Springer, 2002.
- [24] I. N. Bronštejn, editor, *Handbook of mathematics*, 4. ed. (Springer, 2004).

Erklärung

Ich versichere, dass ich diese Arbeit selbstständig verfasst und keine anderen als die angegebenen Quellen und Hilfsmittel benutzt habe.

Heidelberg, den ...